Ab-initio multiplet calculation of oxygen vacancy effect on Ti-L2,3 electron energy loss near edge structures of BaTiO3

S. Ootsuki, H. Ikeno, Y. Umeda, H. Moriwake, A. Kuwabara et al.

Related Articles

High resolution electron energy loss spectroscopy of clean and hydrogen covered Si(001) surfaces: First principles calculations
J. Chem. Phys. 137, 094701 (2012)

Nazca Lines by La ordering in La2/3−xLi3xTiO3 ion-conductive perovskite
Appl. Phys. Lett. 101, 073903 (2012)

Dipolar transformations of two-dimensional quantum dots arrays proven by electron energy loss spectroscopy
J. Appl. Phys. 112, 024105 (2012)

Tuning the surface plasmon on Ag(111) by organic molecules
J. Appl. Phys. 112, 023302 (2012)

A study of the effect of iron island morphology and interface oxidation on the magnetic hysteresis of Fe-MgO (001) thin film composites
J. Appl. Phys. 112, 013905 (2012)

Additional information on Appl. Phys. Lett.

Journal Homepage: http://apl.aip.org/

Journal Information: http://apl.aip.org/about/about_the_journal

Top downloads: http://apl.aip.org/features/most_downloaded

Information for Authors: http://apl.aip.org/authors

Ab-initio multiplet calculation of oxygen vacancy effect on Ti-L$_{2,3}$ electron energy loss near edge structures of BaTiO$_3$

S. Ootsuki,[1,2,a)] H. Ikeno,[3] Y. Umeda,[1] H. Moriwake,[4] A. Kuwabara,[4] O. Kido,[1] S. Ueda,[1] I. Tanaka,[3,4] Y. Fujikawa,[1] and T. Mizoguchi[2,a)]

[1]*Application & Analysis Center, TDK Corporation, 570-2 Matsugashita, Minamihatori, Narita City, Chiba 286-8588, Japan*
[2]*Institute of Industrial Science, The University of Tokyo, 4-6-1, Komaba, Meguro, Tokyo 153-8505, Japan*
[3]*Department of Materials Science and Engineering, Kyoto University, Yoshida, Sakyo, Kyoto 606-8501, Japan*
[4]*Nanostructure Research Laboratory, Japan Fine Ceramics Center, Nagoya 456-8587, Japan*

The effect of oxygen vacancy on Ti-L$_{2,3}$ electron energy-loss near-edge structures (ELNES) of BaTiO$_3$ was theoretically investigated through *ab initio* multiplet calculation. The presence of an oxygen vacancy influences spectral features not only at the nearest neighbor Ti site but also at Ti sites further from the oxygen vacancy. The effects of different oxygen vacancy concentrations were also investigated. Based on this study, it was concluded that the detection limit for oxygen vacancy with Ti-L$_{2,3}$ ELNES is approximately 1%. © *2011 American Institute of Physics*. [doi:10.1063/1.3663543]

BaTiO$_3$ is used as the dielectric layers in the multilayer ceramic capacitors (MLCC).[1] The MLCC device is usually heated in a reduction atmosphere during the fabrication process, and oxygen vacancies are introduced within the BaTiO$_3$ layers. This oxygen vacancy has been known to influence the insulating property of the BaTiO$_3$ layers.[2–6] Thus, identification and control of the oxygen vacancy in the BaTiO$_3$ layers are crucial for the MLCC devices.

To identify oxygen vacancy in BaTiO$_3$ and related perovskite type compounds, Ti-L$_{2,3}$ electron energy-loss near-edge structures (ELNES) observed with transmission electron microscopy (TEM) have been employed.[7–13] It is known that the L$_3$ and L$_2$ edges are each split into two main peaks in the Ti-L$_{2,3}$ ELNES of bulk BaTiO$_3$ (peaks A, B, C, D in Fig. 2).[7–13] When oxygen vacancies are introduced, the splitting between those two peaks at the Ti-L$_3$ edge (peaks A and B in Fig. 2) and the Ti-L$_2$ edge (peaks C and D in Fig. 2) becomes less apparent.[7,8,11,13] These spectral changes have been interpreted as the valency change of Ti from +4 to +3, based on comparisons with the experimental spectra of reference compounds.

However, the oxygen vacancy induces not only extra electron but also structural distortions, and so the effect of the oxygen vacancy on the nearest neighbor Ti site is different from that on Ti sites further away from the oxygen vacancy. Such realistic effects of the oxygen vacancy on the Ti-L$_{2,3}$ ELNES have not been investigated so far. In addition, how well the oxygen vacancy can be detected by the Ti-L$_{2,3}$ ELNES has not been fully understood. The lack of such basic knowledge is mainly because of the absence of good theoretical tools for calculating the transition metal (TM) L$_{2,3}$ ELNES. For simulations of TM-L$_{2,3}$ ELNES, the strong electronic correlation between the core-hole and excited electrons must be properly taken into account, which is beyond the ordinary one-particle density functional calculations.[14]

Recently, Ikeno *et al*. developed an *ab initio* multiplet calculation code for the L$_{2,3}$ edges of TMs.[14–19] In this paper, the Ti-L$_{2,3}$ ELNES of BaTiO$_3$ are theoretically investigated by the *ab initio* multiplet method. Moreover, the effects of the oxygen vacancy on the spectrum and the ability of Ti-L$_{2,3}$ ELNES to detect oxygen vacancy are discussed.

Theoretical calculation of Ti-L$_{2,3}$ ELNES was performed by the *ab initio* multiplet method that is based on the relativistic configuration-interaction theory.[16,17] The calculation was performed with six- or seven-atom clusters embedded in an array of point charges to include the effects of the Madelung potential of BaTiO$_3$. The theoretical transition energy was separately calculated by the Slater transition-state method.

The atomic arrangements around each oxygen vacancy were optimized by a first-principles projector augmented plane wave (PAW) calculation implemented in the Vienna *Ab initio* Simulation Package (VASP) code.[20] The effect of oxygen vacancy on the Ti-L$_{2,3}$ ELNES was investigated using cubic-BaTiO$_3$. 135-atom supercells were used, and all atoms in the supercells were allowed to be relaxed. The optimized positions were used as those of the atoms in the clusters and those of the point charges of the Madelung potentials. To know the effect of extra electron introduced by the oxygen vacancy, both neutral and charged oxygen vacancies were calculated in the models with and without an extra electron.

In the cluster calculation, the effects of the extra electron induced by the oxygen vacancy were simulated by taking into account the change in the valency of the nearest neighbor Ti site to the oxygen vacancy. Namely, when the extra electron is present and localized to the oxygen vacancy, the closest Ti to the oxygen vacancy is considered a Ti^{3+} ion, whereas those further from the oxygen vacancy are considered Ti^{4+} ions. On the other hand, if the extra electron is far away from the oxygen vacancy, all Ti ions were set to Ti^{4+}.

Figure 1 shows an optimized atomic configuration around the oxygen vacancy. Atomic displacements from

a)Authors to whom correspondence should be addressed. Electronic addresses: sootsuki@jp.tdk.com and teru@iis.u-tokyo.ac.jp.
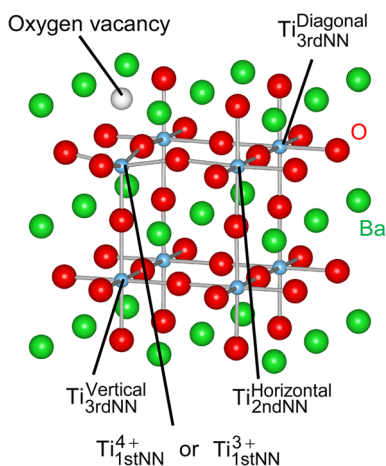
FIG. 1. (Color online) Structure of BaTiO$_3$ with oxygen vacancy and Ti positions of calculation.

–4% to 10% are introduced by the oxygen vacancy.[21,22] In addition, the effect of the extra electron on the lattice relaxation is approximately 1%.[21,22] The Ti-L$_{2,3}$ ELNES were calculated from Ti sites as shown in Fig. 1.

Figure 2 shows Ti-L$_{2,3}$ ELNES of cubic and tetragonal BaTiO$_3$. The experimental spectrum of tetragonal BaTiO$_3$ is shown in the same figure. The experimental spectrum was taken by TEM (JEOL 2200FS with Omega filter), and the energy resolution was around 1 eV. It can be seen in Fig. 2 that the present *ab initio* multiplet calculation reproduces the experimental spectrum well. It is also found that the calculated Ti-L$_{2,3}$ ELNES of cubic and tetragonal BaTiO$_3$ are almost identical. A high energy resolution of better than 0.1 eV is clearly necessary to distinguish between the two different structures merely by Ti-L$_{2,3}$ ELNES.

Figures 3(a) and 3(b) show, respectively, the calculated Ti-L$_{2,3}$ ELNES of the vacancy models without and with an extra electron, namely, with Ti^{4+} or Ti^{3+}. With respect to the oxygen vacancy, Ti-L$_{2,3}$ ELNES were calculated for the nearest neighboring Ti sites (Ti$^{4+}_{1stNN}$ or Ti$^{3+}_{1stNN}$), second nearest neighboring Ti sites (Ti$^{Horizontal}_{2ndNN}$), and third nearest neighboring Ti sites (Ti$^{Vertical}_{3rdNN}$ and Ti$^{Diagonal}_{3rdNN}$). In the case of Ti$^{4+}_{1stNN}$, the spectrum shifts to lower energy and peaks B and D are each split. This peak splitting and spectral shift can be ascribed to dangling-bond formation and decreased Ti ionicity, respectively. In the case of Ti sites further away from the
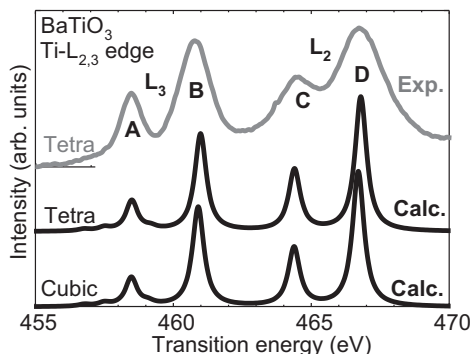

FIG. 2. Experimental Ti-L$_{2,3}$ ELNES of tetragonal BaTiO$_3$ and theoretical Ti-L$_{2,3}$ ELNES of cubic and tetragonal-BaTiO$_3$.
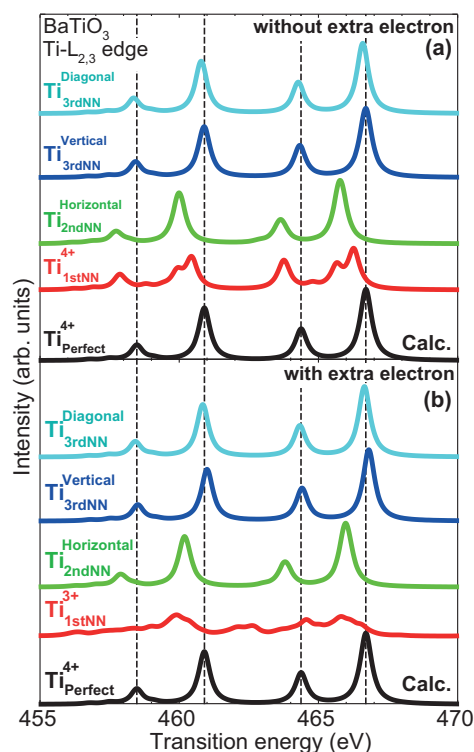

FIG. 3. (Color online) Theoretical Ti-L$_{2,3}$ ELNES of the perfect BaTiO$_3$ and the Ti near oxygen vacancy (a) without and (b) with extra electron.

oxygen vacancy, the spectra are similar to that of perfect BaTiO$_3$, though the spectrum of the Ti$^{Horizontal}_{2ndNN}$ site is shifted to lower energy by 0.9 eV. By analyzing the chemical bonding, it was found that the Ti$^{Horizontal}_{2ndNN}$ site has lower ionicity than other sites, indicating that the oxygen vacancy influences the electronic structure at the Ti$^{Horizontal}_{2ndNN}$ site. Although the spectra of the Ti$^{Vertical}_{3rdNN}$ and Ti$^{Diagonal}_{3rdNN}$ sites are slightly shifted to higher and lower energy, respectively, the magnitude of either shift is almost negligible.

By introducing an extra electron into the nearest neighbor Ti site, the spectral features are completely changed (Ti$^{3+}_{1stNN}$ site). The spectrum features correspond well to experimental spectrum of Ti^{3+} compounds.[11–13,23] However, it is found that the effect of the extra electron does not reach the Ti sites further away from the oxygen vacancy. Namely, the spectral features of Ti$^{Horizontal}_{2ndNN}$, Ti$^{Vertical}_{3rdNN}$, and Ti$^{Diagonal}_{3rdNN}$ are almost identical to those without the extra electron (Figs. 3(a) and 3(b)). From Figs. 3(a) and 3(b), it is found that both structural distortion and extra electron induced by the oxygen vacancy mainly affect to close Ti to the oxygen vacancy. This localized effects can be ascribed to that the Ti-L$_{2,3}$ edge is caused by spatially localized orbitals, Ti-2p and 3d.

To consider the oxygen vacancy concentration, a weighted sum of spectra was calculated from the relation that a lone oxygen vacancy is surrounded by eight Ti$^{Diagonal}_{3rdNN}$ ions, eight Ti$^{Horizontal}_{2ndNN}$ ions, two Ti$^{Vertical}_{3rdNN}$ ions, and two Ti$^{4+}_{1stNN}$ or Ti$^{3+}_{1stNN}$ ions. The much further Ti sites were considered the same as those in perfect BaTiO$_3$. By taking these conditions into account, the effect of oxygen vacancy was simulated with different vacancy concentrations of 0.52%, 1.04%, and 1.56%.
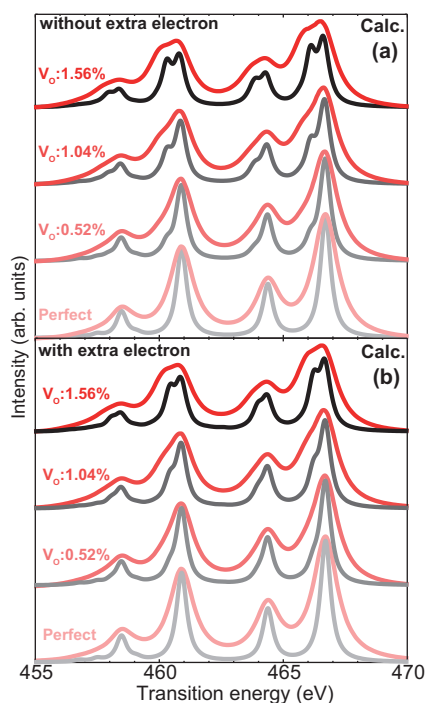
FIG. 4. (Color online) Linear combine spectra of Ti-L$_{2,3}$ of BaTiO$_3$ that include oxygen vacancy(:Vo). Broadening width of the black (thick) and red (thin) lines are 0.5 eV and 1.2 eV, respectively. (a) Ti next to oxygen vacancy is +4 (without extra electron), (b) Ti next to oxygen vacancy is +3 (with extra electron). Deep and light red and gray colors mean high and low concentrations, respectively.

The spectra simulated with different oxygen concentrations are shown in Fig. 4. The calculated spectra were broadened with different broadening factors of 0.5 eV and 1.2 eV to represent the spectral changes in experiments with different energy resolutions. It is clearly found that spectral features are changed by the presence of the oxygen vacancy. In particular, small shoulders appear at the lower energy sides of peaks B and D when the oxygen vacancy concentration exceeds 1%, and those peaks become doublets when the concentration is 1.5%. Although these extra features are less apparent with low energy resolution, the present theoretical calculation suggests that the Ti-L$_{2,3}$ ELNES affords the potential to identify a 1% oxygen vacancy by observing the spectrum with high energy resolution. This detection limit obtained by the present calculation is nicely consistent with that proposed by Muller *et al.* from experiments.[11]

From Figs. 3(a), 3(b), 4(a), and 4(b), it is found that the effect of the extra electron on the averaged Ti-L$_{2,3}$ ELNES is very small, except that the local Ti$_{1stNN}^{4+}$ and Ti$_{1stNN}^{3+}$ yield largely different spectral features. This is because the nearest neighboring Ti sites are four times smaller in number than the second nearest neighboring Ti sites. The spectral changes described above can thus mainly be ascribed to the relatively large chemical shift of the Ti-L$_{2,3}$ ELNES from the second nearest neighboring Ti sites, Ti$_{2ndNN}^{Horizontal}$. That is, the spectral changes in Ti-L$_{2,3}$ ELNES caused by the presence of the oxygen vacancy result from not only the nearest neighboring Ti sites but also the neighboring Ti sites further away from the oxygen vacancy.

Finally, it should be mentioned that Mizoguchi *et al.* and Shao *et al.* discussed the effect of the extra electron,

namely Ti^{3+}, to the Ti-L$_{2,3}$ edge.[14,23] From their results, more than 10% ~ 20% of Ti^{3+} is necessary to observe clear spectrum changes. And the spectral changes induced only by the extra electron mainly appear around the first and third peaks of Ti-L$_{2,3}$ edge, while that by the structural distortion appear around the second and fourth peaks (Fig. 4). By the presence of oxygen vacancy, both extra electron and structural distortions are introduced. Present study demonstrated that consideration of both effects is indispensable to correctly interpret the spectrum.

In summary, the effect of oxygen vacancy on the Ti-L$_{2,3}$ ELNES of BaTiO$_3$ was investigated through *ab initio* multiplet calculation. It was found that spectral differences between cubic and tetragonal BaTiO$_3$ are quite small. From the present analysis, it was concluded that those Ti sites that are further away exert a greater influence on the spectral. Specifically, it was concluded that Ti-L$_{2,3}$ ELNES has the potential to detect an oxygen vacancy concentration of 1%.

[1]M. Randall, D. Skamser, T. Kinard, J. Qazi, and A. Tajuddin, "Thin Film MLCC," CARTS 2007 Symposium Proceedings, Albuquerque, NM, 26–29, March 2007.
[2]T. Baiatu, R. Waser, and K.-H. Härdtl, J. Am. Ceram. Soc. **73**, 1663 (1990).
[3]S. Sato, Y. Nakano, A. Sato, and T. Nomura, Jpn. J. Appl. Phys. **36**, 6016 (1997).
[4]H. Chazono and H. Kishi, Jpn. J. Appl. Phys. **40**, 5624 (2001).
[5]G. Y. Yang, E. C. Dickey, C. A. Randall, D. E. Barber, P. Pinceloup, M. A. Henderson, R. A. Hill, J. J. Beeson, and D. J. Skamser, J. Appl. Phys. **96**, 7492 (2004).
[6]R. Scharfschwerdt, A. Mazur, O. F. Schirmer, H. Hesse, and S. Mendricks, Phys. Rev. B **54**, 15284 (1996).
[7]T. Dechakupt, G. Yang, C. A. Randall, S. Trolier-McKinstryw, and I. M. Reaney, J. Am. Ceram. Soc. **91**, 1845 (2008).
[8]J. Zhang, A. Visinoiu, F. Heyroth, F. Syrowatka, M. Alexe, D. Hesse, and H. S. Leipner, Phys. Rev. B **71**, 064108 (2005).
[9]G. Y. Yang, E. C. Dickey, C. A. Randall, M. S. Randall and L. A. Mann, J. Appl. Phys. **94**, 5990 (2003).
[10]E. Stoyanov, F. Langenhorst, and G. Steinle-Neumann, Am. Mineral. **92**, 577 (2007).
[11]D. A. Muller, N. Nakagawa, A. Ohtomo, J. L. Grazul, and H. Y. Hwang, Nature **430**, 657 (2004).
[12]M. Abbate, F. M. F. de Groot, J. C. Fuggle, A. Fujimori, Y. Tokura, Y. Fujishima, O. Strebel, M. Dmke, G. Kaindl, J. van Elp, B. T. Thole, G. A. Sawatzky, M. Sacchi, and N. Tsuda, Phys. Rev. B, **44**, 5419 (1991).
[13]A. Ohtomo, D. A. Muller, J. L. Grazul, and H. Y. Hwang, Appl. Phys. Lett. **80**, 3922 (2002).
[14]T. Mizoguchi, W. Olovsson, H. Ikeno, and I. Tanaka, Micron **41**, 695 (2010).
[15]H. Ikeno, T. Mizoguchi, Y. Koyama, Y. Kumagai, and I. Tanaka, Ultramicroscopy **106**, 970 (2006).
[16]H. Ikeno, F. M. F. de Groot, E. Staviski, and I. Tanaka, J. Phys.: Condens. Matter. **21**, 104208 (2009).
[17]H. Ikeno, T. Mizoguchi, and I. Tanaka, Phys. Rev. B **83**, 155107 (2011).
[18]H. Ikeno, T. Mizoguchi, Y. Koyama, Z. Ogumi, Y. Uchimoto, and I. Tanaka, J. Phys. Chem. C, **115**, 11871 (2011).
[19]Y. Koyama, T. Mizoguchi, H. Ikeno, and I. Tanaka, J. Phys. Chem. B, **109**, 10749 (2005).
[20]G. Kresse and J. Furthmüller, Phys. Rev. B **54**, 11169 (1996).
[21]H. S. Lee, T. Mizoguchi, T. Yamamoto, S. J. L. Kang, and Y. Ikuhara, Acta Mater. **55**, 6535 (2007).
[22]M. Imaeda, T. Mizoguchi, Y. Sato, H. S. Lee, S. D. Findlay, N. Shibata, T. Yamamoto, and Y. Ikuhara, Phys. Rev. B **78**, 245320 (2008).
[23]Y. Shao, C. Maunders, D. Rossouw, T. Kolodiazhnyi, and G. A. Botton, Ultramicroscopy **110**, 1014 (2010).